NIH Public Access
Author Manuscript
Dev Dyn. Author manuscript; available in PMC 2011 November 1.

Published in final edited form as:
Dev Dyn. 2010 November ; 239(11): 3086–3097. doi:10.1002/dvdy.22428.

Analysis of the Hand1 Cell Lineage Reveals Novel Contributions to Cardiovascular, Neural Crest, Extra-Embryonic, and Lateral Mesoderm Derivatives

Ralston M. Barnes[1], **Beth A. Firulli**[1], **Simon J. Conway**[1], **Joshua W. Vincentz**[1], and **Anthony B. Firulli**[1,*]

[1] Riley Heart Research Center, Wells Center for Pediatric Research, Division of Pediatric Cardiology, Departments of Anatomy and Medical and Molecular Genetics, Indiana Medical School, 1044 W. Walnut St., Indianapolis, IN 46202-5225, USA

Abstract

The basic Helix-Loop-Helix (bHLH) transcription factors Hand1 and Hand2 play critical roles in the development of multiple organ systems during embryogenesis. The dynamic expression patterns of these two factors within developing tissues obfuscate their respective unique and redundant organogenic functions. To define cell lineages potentially dependent upon *Hand* gene expression, we generated a mutant allele in which the coding region of *Hand1* is replaced by *Cre* recombinase. Subsequent Cre-mediated activation of *β-galactosidase* or *eYFP* reporter alleles enabled lineage trace analyses that clearly define the fate of *Hand1*-expressing cells. *Hand1*-driven Cre marks specific lineages within the extra embryonic tissues, placenta, sympathetic nervous system, limbs, jaw, and several cell types within the cardiovascular system. Comparisons between *Hand1* expression and *Hand1*-lineage greatly refine our understanding of its dynamic spatial-temporal expression domains and raise the possibility of novel Hand1 functions in structures not thought to be Hand1-dependent.

Keywords

Hand factors; bHLH; Cre recombinase; lineage analysis

Introduction

A combination of molecular signals and intercellular transcriptional machinery that convey both cell specification cues to pluripotent cells and morphogenic patterning templates to forming organs orchestrate the complex process of embryogenesis. Thus, these specification, differentiation, and morphogenic events are mediated by cell-specific changes in transcription and gene expression. Hand1 is a member of the Twist-family of bHLH proteins that, after forming homo- or heterodimeric transcriptional complexes, bind *cis*-elements to regulate downstream target genes (Firulli, 2003; Barnes and Firulli, 2009; Conway and Firulli, 2009). *Hand1* expression is regulated a tissue specific pattern that is both spatially and temporally dynamic. Throughout development beginning at E7.5 *Hand1* expression is detected throughout lateral and extraembryonic mesoderm populations, asymmetrically in the developing heart, and in a subset of neural crest cells (Cserjesi et al., 1995; Vincentz et al., 2008). Both systemic and conditional gene ablation studies have revealed critical roles

To whom correspondence should be addressed, tfirulli@iupui.edu, (317) 278-5814.

NIH-PA Author Manuscript
NIH-PA Author Manuscript
NIH-PA Author Manuscript

NIH-PA Author Manuscript

NIH-PA Author Manuscript

NIH-PA Author Manuscript

for *Hand1* in placenta, heart and neural crest-derivative development (Firulli et al., 1998; Riley et al., 1998; Morikawa and Cserjesi, 2004; Barbosa et al., 2007)

Specifically, *Hand1* systemic knockouts resulted in a myriad of defects that were complicated by severe extraembryonic and vascular defects that lead to embryonic lethality by E8.5 (Firulli et al., 1998; Riley et al., 1998; Morikawa and Cserjesi, 2004). To circumvent secondary complications due to the imperative requirement for *Hand1* in extraembryonic structure, Cre/LoxP technology has lead to further elucidation of an essential role for *Hand1* during cardiogenesis in patterning the left ventricle and in development of lateral mesoderm derivatives, including the gut (McFadden et al., 2005; Maska et al., 2010). In such complex organ systems, loss of function studies must be coupled with a detailed understanding of gene expression and cell lineage if meaningful conclusions about factor function are to be drawn. Fortunately, the same Cre/loxP technology employed to circumvent embryonic lethality and expand our knowledge of Hand factor function during embryogenesis can also be used to establish these precise cellular lineages.

To better define the origins and ultimate fate of the *Hand1*-expressing cell lineage, we engineered a *Hand1* mutant allele that replaces the *Hand1* coding region with that of a *Cre recombinase* cassette. We show, using *R26R* alleles that express conditionally activatable*β-galactosidase* or *eYFP* in the presence of *Cre Recombinase*, contributions of the *Hand1*-expressing cell lineage within the heart, cardiac neural crest cells (cNCC), jaw, sympathetic nervous system, placenta, limb and a subset of vascular endothelium. We reveal that *Hand1* expression is largely absent from cardiomyocytes derived from the second heart field (SHF) and marks cells of the epicardial, but not endocardial, lineage. Although real-time expression analyses suggest *Hand1*-expression in a limited subset of cNCC, lineage analyses shows that *Hand1*-marked cNCC occupying the cardiac outflow tract (OFT), constitute the majority. Additionally, derivatives of the *Hand1*-expressing lineage include midline structures within the cranial NCC, sympathetic ganglia, and the components of the smooth muscle and submucosal lining of the gut, pancreas, bile duct, and the posterior vein originating from the lateral mesoderm. Limb expression of *Hand1* mRNA is restricted to the proximal lateral mesoderm that contributes to the scapula, while the *Hand1* lineage marks both the zeugopod and autopod of the developing limb buds, progenitors of more distal limb structures. As expected, trophoblast giant cells and placental labyrinthine cells are *Hand1*-derived. Placental labyrinth vascular endothelium and caudal vascular endothelium of the descending dorsal aorta are also marked by the *Hand1*-lineage, indicating that *Hand1* marks unique extraembryonic and caudal subpopulations of endothelial cell progenitors. Taken together, these data reveal that cells of the *Hand1*-expressing lineage contribute to both expected and novel embryonic cell populations supporting a central role for *Hand1* function during early cell specification and morphogenesis.

Results

Generation of *Hand1*$^{EGFPCre\Delta Neo/+}$ mice

To follow the fate of cells that express *Hand1*, we targeted an *eGFPCre* fusion protein expression cassette to the *Hand1* locus in a murine ES cell line via homologous recombination (Fig. 1A). Following neomycin selection, targeting was confirmed in ES cell clones via Southern blot analysis (Fig. 1B). Properly targeted ES cells display a single 10Kb *Cre* cassette-containing *EcoRI* RFLP in the absence of secondary sites of insertion (Fig. 1C). Two targeted ES clones were injected to host blastocysts to generate first chimeric mice and then germline *Hand1*$^{EGFPCre\Delta Neo/+}$ allelic transmission. Removal of the *neomycin* resistance cassette, via intercross with *FLPeR* mice (Farley et al., 2000), resulted in a detectable *Hand1*$^{EGFPCre\Delta Neo/+}$ RFLP size shift (Fig. 1D). Both mouse lines expressed *Cre* identically,

NIH-PA Author Manuscript

NIH-PA Author Manuscript

NIH-PA Author Manuscript

and we thus employed only one of these lines for these studies. *eGFP* mRNA expression, detected via *in situ* hybridization, correlates precisely with that of *Hand1* (Fig. 1E,F). *Hand1*$^{EGFPCre\Delta Neo/+}$ mice are viable and fertile but must be maintained as heterozygotes as homozygotes are null for *Hand1* and thus die embryonically (Firulli et al., 1998).

The *Hand1* Lineage contributes to a subset of the FHF and epicardium

To test the fidelity of the *Cre* expression in *Hand1*$^{EGFPCre\Delta Neo/+}$ mice, we intercrossed *Hand1*$^{EGFPCre\Delta Neo/+}$ males with *Cre Recombinase* conditionally activatable *R26R-β-galactosidase (*β-gal) homozygous female mice and compared β-gal reporter activity with both real-time *Hand1* mRNA expression and β-gal activity from the *Hand1*^{LacZ} allele (Fig. 2). At E9.5, both whole-mount and section analyses shows no significant difference between real-time and *Hand1*-lineage expression (Fig. 2A, C, E, G, I, K). As expected, *Hand1* expression and lineage mark the first heart field (FHF) derived left ventricle, showing little expressional overlap with the *Hand2*-expressing SHF (Morikawa and Cserjesi, 2008). Interestingly, at E10.5 *Hand1*-lineage departs from real-time *Hand1* expression. In whole mount, the entire heart appears to be *Hand1*-lineage positive, which would superficially suggest an upregulation of *Hand1* within the SHF (Fig. 2F). However, section analysis discounts this observation, revealing a right ventricular myocardium largely devoid of LacZ activity (Fig. 2L,Q). Rather, the epicardium is robustly LacZ stained in *Hand1*$^{EGFPCre\Delta Neo/+}$ embryos in contrast to *Hand1*$^{LacZ/+}$ embryos, which show no detectable epicardial LacZ staining (Fig. 2J,P). Thus, cells that expressed *Hand1* during their maturation ultimately contribute to cardiac epicardium.

We then examined E15.5 and adult myocardial tissues to assess the contributions of the *Hand1*-lineage to both the late embryonic and the fully formed heart (Fig. 3A–B). At these stages, the *Hand1*-lineage continues to mark a portion of the inner wall of the interventricular septum (IVS) and the left ventricular myocardium. LacZ staining is not detected in adult atrial cardiomyocytes, indicating that the *Hand*-lineage does not mark cardiomyocytes within the entire FHF, but only a subset that contributes to the left ventricle. Consistent with earlier time points, SHF derived right ventricular myocardium shows no evidence of *Hand1*-expression and, with the exception of a small population of SHF derived cardiomyocytes within the myocardial cuff, there is a near exclusion of *Hand1* expression from SHF derived myocardium (Srivastava et al., 1995; McFadden et al., 2000).

Both *in situ* hybridization and *Hand1*^{LacZ} staining fail to detect *Hand1* within the endocardial or epicardial lineages. We intercrossed *Hand1*$^{EGFPCre\Delta Neo/+}$ males with *Cre Recombinase* conditionally activatable *R26R-eYFP (*eYFP) homozygous female mice and performed immunohistochemistry to detect co-expression of Flk1 and eYFP to carefully examine whether the *Hand1*-lineage contributes to the endocardium or coronary endothelium (Fig 3C–H). Consistent with the lack of detectable real-time expression, no Flk1-positive endocardial or coronary vessel cells coexpressed eGFP.

LacZ staining of the *Hand1*-lineage was also not detected within the atrial myocardium. Immunohistochemistry for the *Hand1*-lineage did not mark the atrial myocardium, validating this observation (Fig. 3I–K). Together, these data provide a new perspective on the contributions of *Hand1*-expressing lineages to the heart where, with the exception of the myocardial cuff, *Hand1* is excluded from SHF myocardium, is restricted to a ventricular subpopulation of the FHF, and marks both the progenitors and derivatives of the proepicardial organ and epicardium.

NIH-PA Author Manuscript

NIH-PA Author Manuscript

NIH-PA Author Manuscript

The *Hand1*-lineage marks specific subpopulations of cranial, cardiac and trunk neural crest, but not vagal/sacral neural crest

Hand1 and *Hand2* expression is observed within subpopulations of cranial, cardiac, trunk, and vagal/sacral NCCs that contribute to the jaw, cardiac OFT, sympathetic nervous system and enteric nervous system, respectively (Abe et al., 2002; Yanagisawa et al., 2003; Barbosa et al., 2007; Morikawa et al., 2007; Hendershot et al., 2008; Morikawa and Cserjesi, 2008; Holler et al., 2010). This expression can be observed in whole mount *Hand1*^{LacZ} expression at E12.5 (Fig. 4A). Craniofacial expression of *Hand1* at E12.5 is restricted to the midline of both the developing tongue and the mandibular process, and at E14.5 it is still expressed in the midlines of both the tongue and the Meckel's cartilage in the mandible (Fig. 4B, C, E, and F). Comparisons of real-time *Hand1* expression to the *Hand1* craniofacial lineage at E14.5 show that the *Hand1*-lineage marks a wider subset of tissue within the tongue and the entirety of Meckel's cartilage in the mandible (Fig. 4D, G). This suggests that *Hand1* may influence formation of midline features of both the tongue and lower jaw.

Hand1 real-time expression within the OFT and pharyngeal arches of E10.5 mouse embryos is subtly distinct from that of the *Hand1*-expressing cNCC lineage (Fig 4H, I). Medial cNCC within the forming aortico-pulmonary septum show an indistinguishable distribution of *Hand1*-expressing/marked cells. However, *Hand1*^{LacZ} expression is observed in approximately 50% of cNCC occupying the OFT, while almost all of these cells are marked as having derived from the *Hand1*-lineage suggesting that *Hand1* real-time expression is downregulated as cNCC migrate into the OFT (Fig.4B). This finding is consistent with previously published observations (Vincentz et al., 2008).

Hand1 expression marks trunk NCC-derived neurons within the sympathetic ganglia (Cserjesi et al., 1995; Hollenberg et al., 1995; Firulli et al., 1998). Comparison of *Hand1* expression with that of the *Hand1*-lineage shows little variation (Fig. 4J, K). *Hand1*$^{Lacz/+}$ E18.5 embryos show robust β-gal staining within the sympathetic chain (Fig. 4J), and this expression persists in adults (data not shown). *Hand1*-lineage is consistent with this expression (Fig. 4K).

Finally, we looked at the *Hand1*-lineage within the vagal/sacral NCC-derived cells of the enteric nervous system and gut at E12.5 and 14.5 (Fig. 4L–N, P–R). *Hand1* expression was found in the smooth muscle component of the midgut and hindgut. At E14.5, the *Hand1*-lineage robustly marks both the submucosa of the duodenum, a smooth muscle cell subpopulation surrounding the muscilaris externa, and the outer connective adventitia. The *Hand1*-lineage is absent from villus epithelium. Additionally, the *Hand1*-lineage is detected within the posterior vein and the bile duct, as well as the surrounding connective tissue. Comparison of the *Hand1*-lineage to the *Wnt1*-lineage at E14.5 indicates that the *Hand1* lineage is excluded from the NCC components of the enteric nervous system but does mark lateral mesoderm structures of the gut (Fig. 4Q, S)

The *Hand1*-lineage shows varying contributions to the developing fore- and hindlimbs

Hand1 is expressed, beginning at E11.5, within the anterior-ventral domain of the developing mouse limb and, by E13.5, is restricted to digit 1 (Fernandez-Teran et al., 2003). *Hand1* is also expressed within the lateral mesoderm medial to the forming limb buds. Compared to *Hand2*, limb expression *Hand1* is greatly restricted; however, expression of these two related factors does partially overlap (Fernandez-Teran et al., 2003; Firulli et al., 2005).

Forelimb expression of *Hand1* at E9.5 and E10.5 appears in the lateral mesoderm underlying the forelimb bud (Fig. 5A,E). Lineage analysis marks this lateral mesoderm population that contributes to limb bud mesenchyme (Fig. 5B). At E10.5 the *Hand1*-lineage marks a subset

NIH-PA Author Manuscript

NIH-PA Author Manuscript

NIH-PA Author Manuscript

of cells that contribute predominantly to the ventral side of the limb bud, indicating that *Hand1*-positive cells in the lateral mesoderm contribute to limb bud development in a pattern-specific manner (Fig. 5F).

Meanwhile, hindlimb expression of *Hand1* at E9.5 marks both the lateral mesoderm and the ventral mesenchyme of the limb bud (Fig. 5C). The *Hand1*-lineage at E9.5 marks, in addition to the ventral and lateral mesoderm derived cells, a considerable subset of mesenchymal cells occupying the dorsal compartment of the limb bud (Fig 5D). At E10.5, *Hand1* hindlimb expression becomes restricted to the lateral mesoderm, while we see a broad expansion of the *Hand1*-lineage throughout the hindlimb mesenchyme. This indicates that both dorsal and ventral hindlimb mesenchyme receive an early and substantial contribution of *Hand1*-expressing cells.

Hand1 expression is considerably downregulated within the limb bud by E10.5. Whole mount analysis of $Hand1^{LacZ}$ at later stages confirms, as has been previously reported, a late domain of expression at E12.5 in both the fore- and hindlimbs (Fig. 5I,K) (Fernandez-Teran et al., 2003). This expression of *Hand1* is downregulated in the limb by E14.5 (Fig. 5M, N). Lineage analyses at E12.5 and E14.5 confirm contribution of *Hand1*-expressing cells to the limbs with, as expected, comparatively more extensive staining in the hindlimb, (Fig. 5J, L, N, P). Importantly, these experiments indicate that there are two separate expression domains of *Hand1* within the developing limb. First, there is an early expression domain, detectable during stylopod formation, largely within the lateral mesoderm and the ventral forelimb bud. Surprisingly, derivatives of these early *Hand1*-expressing cells contribute extensively to the limb bud mesenchyme. Second, there is a late expression domain of *Hand1* that is crucial for digit formation during autopod maturation (Fernandez-Teran et al., 2003). Together, these data indicates that the expression and contribution of *Hand1* during limb formation is more dynamic than previously thought.

The *Hand1*-lineage contributes to the extraembryonic mesoderm and trophoblasts during placental development

Hand1 null mice die between 8.5 and 9.5 due to defects in extraembryonic and vascular tissues (Firulli et al., 1998; Riley et al., 1998; Morikawa and Cserjesi, 2004). Contributions of the *Hand1*-lineage to the placenta and associated vasculature were assessed at E9.5, and E14.5 (Fig. 6). As expected, at E9.5 the *Hand1*-lineage marks the chorion, allantois, yolk sac, and trophoblast giant cells (Fig. 6A–D), and is not observed within the decidua (Fig. 6A, C). At E14.5, after the specific layers of the placenta have formed, the *Hand1*-lineage contributes, in addition to yolk sac and chorion, to the amnion, both the endothelium and the smooth muscle of the umbilical vein, Wharton's jelly, which surrounds and insulates the developing umbilical chord, the vitiline vessels, a heterogeneous cell population within the placental labyrinth and the trophoblasts within the anterior domain of the spongy layer (Fig. 6E–H). To identify these *Hand1*-lineage-postive cells within the labyrinth, immunohistochemistry was performed using eGFP, Flk1, and αSMA antibodies at E12.5 (Fig. 6I–P). A complete overlap of eGFP and Flk1 immunoreactivity is observed, suggesting that the *Hand1*-lineage marks the vascular endothelium, where as the complimentary pattern of αSMA suggests that smooth muscle within this domain derives from cells independent of *Hand1*-expression. Real-time *Hand1* expression is indistinguishable from *Cre* expression at these stages (data not shown). Taken together, these data show that cells which do express or which have expressed *Hand1* compose nearly all trophoblasts and components of the extraembryonic vasculature as well as a significant portion of the labyrinth endothelium.

NIH-PA Author Manuscript

NIH-PA Author Manuscript

NIH-PA Author Manuscript

Hand1 marks vascular structures derived from lateral mesoderm

At E9.5 and 10.5, real-time *Hand1*^{LacZ} staining clearly shows lateral mesoderm-restricted expression (Fig. 7A–B). In contrast, *Hand1*-lineage analysis at these time points reveals cells migrating out of the lateral mesoderm between the somites (Fig. 7C–D). Close examination suggests that these cells are forming the vascular plexus of the intersomitic vessels. CD31 (PECAM) antibody staining confirms that these *Hand1*-lineage cells are vascular endothelium (Fig. 7C–F). Comparison between the *Hand1*, lineage and the *Wnt1-Cre* lineage confirms the *Hand1* lineage marked vascular endothelium is derived from the lateral mesoderm and not the NCC lineage (Fig. 7G–H). No *Hand1*-linage contribution was observed rostral to the forelimb, indicating that the vascular progenitors of these vessels are independent of *Hand1* expression (data not shown).

To more precisely characterize *Hand1* vascular contributions, we examined the *Hand1*-lineage within caudal sections of E9.5 day embryos (Fig. 8). *Hand1*-linage cells are readily detectable in the caudal endothelium of the dorsal aorta (Fig. 8B, D). Interestingly, at E14.5 the Flk1-positive endothelium of the distal dorsal aorta (Fig. 8G, K) is composed of a mix of both *Hand1*-lineage, detected by expression of eGFP (Fig. 8G, K), and non-lineage cells (Fig. 8H, L). *Hand1*-lineage cells are not observed within the endothelium of the proximal dorsal aorta (data not shown) but can be observed in small populations within the vessels that increase in number moving caudally from the forelimb. Interestingly, the *Hand1*-lineage also marks a small population of blood cells (Fig. 8D, L). It is likely that the extensive *Hand1*-expressing cells within extraembryonic structures and the lateral mesoderm respectively contribute to blood islands within the yolk sac and, potentially, blood cells that populate the liver. Given that the *Hand1*-lineage contributes to endothelium of both the intersomitic vessels and the dorsal aorta, we conclude that components of the caudal vasculature and some hematopoietic cells derive from *Hand1*-expressing progenitors.

Discussion

bHLH proteins depend upon dimer formation to bind DNA and regulate gene expression; thus, defining where these factors are expressed is necessary to evaluate their mechanistic roles during organogenesis. The dynamic spatiotemporal expression of Twist family bHLH proteins renders an understanding of their mechanistic and functional roles as dictated by dimer partner choices a significant challenge. Although loss-of-function analyses in both systemic and conditional models have provided insights into the role of Hand1 in extraembryonic, cardiac, and NCC derived tissues, the expression data available is still limiting.

Here, we have created a *Hand1* allele that permanently marks all *Hand1*-expressing cells, enabling their developmental fates to be monitored. In some instances, such as in extraembryonic structures, observations of the *Hand1*-lineage completely correlate with real-time expression; however, observations of lineage-marked cells clearly refine and expand real-time expression data, revealing novel potential domains of *Hand1* function. This is exemplified in the developing myocardium by the near exclusive restriction of *Hand1*-marked cells to ventricular structures derived from the FHF. The *Hand1*-lineage marks the outer curvature of the left ventricle, is absent from the atria, and is not expressed at significant levels within the SHF-derived right ventricle, which robustly expresses the related factor *Hand2*. As *Hand1* expression in the FHF myocardium expands, *Hand2* expression dominates within the SHF cells that are migrating into the heart from both atrial and venous poles. *Hand1* is clearly expressed and specifically marks the SHF-derived myocardium within the myocardial cuff, a tight ring of myocardium in direct contact with the forming OFT. The *Hand1*-lineage does not contribute to the endocardium, whereas *Hand2* is expressed within these cells. Therefore, *Hand1* and *Hand2* expression overlaps

NIH-PA Author Manuscript

NIH-PA Author Manuscript

NIH-PA Author Manuscript

within FHF derived myocardium of the left ventricle beginning at E8.5 and within the SHF derived myocardial cuff at E9.5. Expression within other SHF-derived myocardium and endocardium is exclusively defined by *Hand2*.

The *Hand1*-lineage analyses potentially reveal a novel role for Hand1 in the formation of the epicardium. Comparison of *Hand1*$^{LacZ/+}$ and *Hand1*$^{eGFPCre/+}$ mice up to E9.5 shows no significant variation within the forming heart (Fig. 2). By E10.5, the entire surface of the heart is composed of *Hand1*-lineage marked cells, whereas real time *Hand1* expression is not observed. We also observed that coronary smooth muscle and cardiac fibroblasts, but not coronary endothelium, are derived from *Hand1*-expressing cells. Given that the epicardium gives rise to both cardiac fibroblasts and the smooth muscle of the coronaries, but not coronary endothelium, this supports the conclusion made by Red-Horse et al., which shows that coronary endothelium is not a derivative of the epicardium, but comes from endothelial progenitors within the sinus venosae (Red-Horse et al.). Exploring the role Hand1 plays in defining epicardial progenitors will be an interesting and informative area to pursue.

In addition to expression in the heart, *Hand1*-lineage contributes to the cardiac OFT, jaw, sympathetic nervous system and lateral mesodermal derivatives of the gut. Within the OFT, *Hand1*-lineage analysis suggests that the majority of cNCC within the OFT, at some point in their emigration, expressed *Hand1*; however, real-time expression at E10.5 shows that only a subset (approximately 50%; (Vincentz et al., 2008) actively express *Hand1* transcript (Fig. 4). These cNCC are interesting in that they coexpress *Twist1* and *Hand2*, and although deletion of *Hand1* in the NCC via *Wnt1-Cre* is reported to show no obvious OFT phenotypes (Barbosa et al., 2007), the *Hand1 and Hand2* real-time expressing cells are observed to selectively show defective cell adhesion on the *Twist1* null background (Vincentz et al., 2008). Given that gene dosage relationships between these potential dimer partners are evident, looking at more compound relationships between these factors using the *Hand1* eGFP-Cre driver could be informative.

In the sympathetic ganglia, *Hand1* expression is observed as early as E11.5. *Hand2* expression precedes this upregulation. *Wnt1-Cre* mediated *Hand2* deletion results in a loss of *Hand1* expression (Morikawa et al., 2007). *Hand1* expression within the sympathetic ganglia persists into adulthood and we observe no significant differences between real-time and *Hand1*-lineage expression patterns. Similarly *Hand1*-lineage analysis of the enteric nervous system does not show deviation from that of real-time *Hand1* expression.

Within the cranial NCC, Hand1, in conjunction with dosage modifiers such as Hand2, impairs growth of the distal midline mesenchyme (Barbosa et al., 2007). Real-time *Hand1* expression marks the midline of the developing mandible and the midline of the tongue. The *Hand1*-lineage clearly marks the midline mesenchyme of the frontal processes of the face throughout all Meckel's cartilage derivatives. Additionally, the *Hand1*-lineage appears to contribute to a more extensive domain in the midline region of the tongue. This suggests that either *Hand1* expression becomes restricted during the differentiation process of the midline cranial neural crest cells or that the *Hand1*-lineage migrates outward from the site of active *Hand1* expression in the midline cranial neural crest.

Ectopic expression of Hand factors within the limb results in preaxial polydactyly (Fernandez-Teran et al., 2000; McFadden et al., 2002 Fernandez-Teran, 2003 #2350). Mechanistically, this phenotype is also a consequence of *Hand*/*Twist* gene dosage, where functional antagonism between Twist1 and Hand proteins mediated by dimer partner choice causes a variety of limb abnormalities (Firulli et al., 2005; Firulli et al., 2007). Real-time expression of *Hand1* within the mouse limb is restricted to the anterior-ventral area of mesoderm at mid-level in the proximo-distal axis (Fernandez-Teran et al., 2003). In chick,

NIH-PA Author Manuscript

NIH-PA Author Manuscript

NIH-PA Author Manuscript

this expression is accompanied by expression within the ventral lateral mesoderm of the forming limbs, but this domain was not detected in the mouse. Interestingly, *Hand1*-lineage analysis defines forelimb vs. hindlimb differences. Forelimb *Hand1*-lineage expression appears to mirror real-time expression, with the exception that the increased sensitivity of the R26R reporter reveals *Hand1*-activty within the ventral mesoderm of the forming forelimb. The *Hand1* forelimb lineage experiment reveals the early contributions of *Hand1* expressing lateral mesoderm to help establish dorso-ventral patterning (Johnson and Tabin, 1997). Molecularly, dorso-ventral patterning is established as an essential modular cascade within limb patterning and hobbling of this cascade models clinical limb defects (Grieshammer et al., 1996; Chen et al., 1998; Ahn et al., 2001; Chen and Johnson, 2002). Hindlimb contributions appear much more extensive than those revealed by real-time analyses and likely reflect the lateral mesodermal origin of the hindlimb mesenchyme. Although Hand1 function within the limbs is not well established, especially when compared to its putative dimer partners *Hand2* and Twist, the differential activity of this *Cre* allele could help define its role in limb morphogenesis.

The last and perhaps most important role for Hand1 is its functions in extraembryonic tissues and its role in the specification and differentiation of trophoblast giant cells (Firulli et al., 1998; Riley et al., 1998; Morikawa and Cserjesi, 2004). *Hand1* is persistently expressed in these extraembryonic tissues and trophoblasts cells and thus the *Hand1*-lineage does not add any additional insight. This expression raises the largest caveat with this *Cre*-driver in that, if extraembryonic expression is encountered, this *Cre* driver line would not be optimal for use in looking at gene ablation in embryonic structures. That being said, if potential targets for conditional deletion within the embryo are expressed in primary myocardium, post-migratory neural crest, lateral mesoderm and or hindlimb mesenchyme, use of this reagent could prove useful in dissecting mechanism via the conditional loss-of-function approach.

Experimental Procedures

Targeting *Hand1* and Generation of Mice

To construct the targeting vector, a 3.4Kb eGFPCre cassette (kindly provided by Dr. Simon J. Conway) was isolated with a *XhoI*/*HindIII* digest and ligated into pBluescript SK+. A 3.0Kb *BstEII* fragment, cloned into pBluescript SK(+), upstream from the *Hand1* translational initiation codon was isolated with a *XhoI* digest and ligated 5’ of the eGFPCre cassette. A 1.75Kb *Frt*-flanked neomycin cassette was isolated from ploxFlpneo (provided by Thomas Saunders U. Michigan) with an *EcoRI/NotI* digest and ligated 3’ of the eGFPCre cassette. A 1.6Kb *SalI*/*HindIII* fragment, cloned into pBluescript SK(+), that extended from within the first intron of the gene into the second exon was isolated with a *NotI* digest and cloned 3’ of the neomycin cassette. The targeting vector was linearized with *XhoI*, prior to electroporation into CCE 916 wildtype ES cells, and plated onto G418-resistant STO feeder layers. Following positive selection with G418, individual ES colonies were isolated and analyzed by Southern blot for homologous recombination at the *Hand1* locus, as previously described (Firulli et al., 1998). Homologous recombination was observed at a frequency of 1:4 in the 150 ES cell clones analyzed. Four independent clones were injected into blastocysts obtained from C57/B6 mice, which were subsequently implanted into pseudopregnant Swiss foster females. Chimeras that were obtained transmitted the *Hand1* mutation through the germline and the resulting offspring were intercrossed with homozygous $R26^{Fki}$ (FLPeR) mice on a pure 129/SvJaeSor genetic background to permanently delete the neomycin cassette. Offspring were then intercrossed to remove the $R26^{Fki}$ allele.

NIH-PA Author Manuscript

NIH-PA Author Manuscript

NIH-PA Author Manuscript

Genotyping

ES cell DNA, as well as tail genomic DNA from *Hand1*$^{EGFPCre\Delta Neo/+}$ mice, were analyzed for the *Hand1* mutation by Southern-blot analysis (Firulli et al., 1998). Insertion of the *eGFPCre* and *neo* genes into the *Hand1* locus introduced an *EcoRI* site that could be used to distinguish the wild-type and targeted alleles, which yielded 10.0Kb and 4.0Kb fragments, respectively, following Southern analysis of *EcoRI*-digested DNA and hybridization with a labeled *BssHII-XhoI* probe from the region 3' of the targeted mutation. Following removal of the *neo* gene, the 4.0Kb fragment shifted to a 2.25Kb fragment. Since the targeting construct did not contain a negative selection gene, an 861bp *NcoI* fragment from the *eGFPCre* cassette was labeled and hybridized to *EcoRI*-digested DNA, yielding a 10.0Kb band. Ectopic bands were not detected.

ROSA26R-β-gal homozygous mice were genotyped using a probe located 5' of the STOP Flox (provided by Dr. Phillippe Soriano). Southern analysis of *EcoRV*-digested DNA was hybridized with labeled probe and yielded a 3.8Kb band. *ROSA26R-eYFP* were obtained from the Jackson lab and were genotyped using the aforementioned Southern strategy.

Mating Schemes and Histological Preparations

Hand1$^{EGFPCre\Delta Neo/+}$, males were crossed to *Cre Recombinase* conditionally activatable *ROSA26R-β-gal/ eYFP* homozygous female reporter mice (Soriano, 1999; Srinivas et al., 2001). To generate lineage data. *Hand1*^{Lacz} X-gal staining and histological preparations were done as previously described for paraffin embedded sections and whole mounts (Vincentz et al., 2008) For E15.5 and adult heart, embryos/tissues were dissected in PBS and fixed in a 1:1 mixture of 4% paraformaldehyde (PFA) in phospho-buffered saline (PBS) and 1X PBS for 5 minutes at 4°C. Samples were then moved to 30% sucrose in 1X PBS overnight at 4°C. Samples were then cryoprotected and stored at −80°C. Samples were sectioned at 10–20mm and washed for 5 minutes in 1X PBS. Sections were then post-fixed in 0.5% PFA for 2 minutes, rinsed in 1X PBS then washed in 1X PBS for 10 minutes. Slides were then incubated with X-gal solution in the dark at 37°C overnight. Slides were rinsed in 1X PBS and then post-fixed in 4% PFA for 20 minutes and then were washed three times in 1X PBS at room temperature for 5 minutes each. Slides were counterstained with Nuclear Fast Red.

Section RNA *In Situ* Hybridization

Section *in situ* hybridization was performed essentially as previously described (Vincentz et al., 2008). Antisense digoxygenin-labeled riboprobes were transcribed with T7, T3, or SP6 (Roche) following linearization of template DNA.

Immunohistochemistry

Embryos were fixed in 4% PFA overnight then embedded in paraffin or cryoprotected and sectioned at 7–10um. Frozen sections were washed in PBS, blocked in 2% normal serum for 1 hour. A primary antibody for Flk1 (Abcam) α-SMA (Sigma), GFP (Invitrogen), and Flk1 (Abcam) was incubated at 4°C overnight. Secondary antibodies were conjugated with Alexa 488 or 594 (Molecular Probes).

Whole Mount Immunohistochemistry

For whole-mount immunohistochemistry with Rat α-CD31 (BD Pharmingen, Cat# 550274), embryos were collected in 1X PBS and were fixed overnight in 4% PFA. Embryos were rinsed in 1X PBS three times and dehydrated through a methanol gradient (25%, 50%, 75%, 100% twice), and stored at −20°C until use. Embryos were bleached for 1 hour on ice in 5% H_2O_2/methanol. Embryos were then rinsed in 100% methanol for 10 minutes and rehydrated

NIH-PA Author Manuscript

NIH-PA Author Manuscript

NIH-PA Author Manuscript

thru a methanol gradient. The remainder of steps were then carried out at 4' on a nutator. Embryos were washed three times in PBTXX (1X PBS, 1% Triton X-100) and then blocked in PBSMT (1X PBS, 2% nonfat instant skim milk, 0.5% Trition X-100) for 2 hours. The blocking solution was then removed and embryos were incubated overnight in PBSMT with 1' antibody (1:250). The following day, embryos were washed five times in PBSMT for 1 hour each. Embryos were then incubated in PBSMT with Goat α-RAT (ABCAM, Cat# AB7097) 2' antibody (1:250). The following day embryos were washed five times in PBSMT for 1 hour each. Embryos were then washed twice in PBTXX for 10 minutes at room temperature. Embryos were developed using DAB substrate kit (VECTOR, SK-4100).

Clearing of Embryos

Hand1$^{LacZ/+}$ mice, *Hand1*$^{EGFPCre\Delta Neo/+}$ mice, and PECAM immunohistochemistry stained embryos were cleared following dehydration washing embryos in BABB (Benzyl Benzoate:Benzyl Alcohol at a 2:1 concentration). Embryos were photographed with bright field illumination.

Acknowledgments

Grant Sponsor: NIH RO1HL061677-09 1P01HL085098-01A (ABF), and AHA 0815426G (RMB).

We would like to thank Danny Carneyfor technical assistance and Dr. Henry Sucov (UCSC) for providing the *Wnt1*-Cre mouse line. Infrastructural support at the Herman B Wells Center for Pediatric Research is in part supported by the generosity of the Riley Children's Foundation and Division of Pediatric Cardiology.

References

Abe M, Tamamura Y, Yamagishi H, Maeda T, Kato J, Tabata MJ, Srivastava D, Wakisaka S, Kurisu K. Tooth-type specific expression of dhand/HAND2: possible involvement in murine lower incisor morphogenesis. Cell Tissue Res. 2002; 310:201–212. [PubMed: 12397375]

Ahn K, Mishina Y, Hanks MC, Behringer RR, Crenshaw EB 3rd. BMPR-IA signaling is required for the formation of the apical ectodermal ridge and dorsal-ventral patterning of the limb. Development. 2001; 128:4449–4461. [PubMed: 11714671]

Barbosa AC, Funato N, Chapman S, McKee MD, Richardson JA, Olson EN, Yanagisawa H. Hand transcription factors cooperatively regulate development of the distal midline mesenchyme. Developmental Biology. 2007; 310:154–168. [PubMed: 17764670]

Barnes RM, Firulli AB. A Twist of insight, the role of Twist-Family bHLH factors in development. Int J Dev Biol. 2009; 53:909–924. [PubMed: 19378251]

Chen H, Johnson RL. Interactions between dorsal-ventral patterning genes lmx1b, engrailed-1 and wnt-7a in the vertebrate limb. Int J Dev Biol. 2002; 46:937–941. [PubMed: 12455631]

Chen H, Lun Y, Ovchinnikov D, Kokubo H, Oberg KC, Pepicelli CV, Gan L, Lee B, Johnson RL. Limb and kidney defects in Lmx1b mutant mice suggest an involvement of LMX1B in human nail patella syndrome. Nat Genet. 1998; 19:51–55. [PubMed: 9590288]

Conway SJ, Firulli AB. A bHLH Code for Cardiac Morphogenesis. Pediatr Cardiol. 2009 Epub ahead of print.

Cserjesi P, Brown D, Lyons GE, Olson EN. Expression of the novel basic helix-loop-helix gene eHAND in neural crest derivatives and extraembryonic membranes during mouse development. Dev Biol. 1995; 170:664–678. [PubMed: 7649392]

Farley FW, Soriano P, Steffen LS, Dymecki SM. Widespread recombinase expression using FLPeR (flipper) mice. Genesis: the Journal of Genetics & Development. 2000; 28:106–110.

Fernandez-Teran M, Piedra ME, Kathiriya IS, Srivastava D, Rodriguez-Rey JC, Ros MA. Role of dHAND in the anterior-posterior polarization of the limb bud: implications for the sonic hedgehog pathway. Development. 2000; 127:2133–2142. [PubMed: 10769237]

Fernandez-Teran M, Piedra ME, Rodriguez-Rey JC, Talamillo A, Ros MA. Expression and Regulation of eHAND During Limb Development. Dev Dyn. 2003; 226:690–701. [PubMed: 12666206]

NIH-PA Author Manuscript

NIH-PA Author Manuscript

NIH-PA Author Manuscript

Firulli AB. A HANDful of questions: The molecular biology of the HAND-subclass of basic helix-loop-helix transcription factors. Gene. 2003; 312C:27–40. [PubMed: 12909338]

Firulli AB, McFadden DG, Lin Q, Srivastava D, Olson EN. Heart and extra-embryonic mesodermal defects in mouse embryos lacking the bHLH transcription factor Hand1. Nature Genetics. 1998; 18:266–270. [PubMed: 9500550]

Firulli BA, Krawchuk D, Centonze VE, Virshup DE, Conway SJ, Cserjesi P, Laufer E, Firulli AB. Altered Twist1 and Hand2 dimerization is associated with Saethre-Chotzen syndrome and limb abnormalities. Nat Genet. 2005; 37:373–381. [PubMed: 15735646]

Firulli BA, Redick BA, Conway SJ, Firulli AB. Mutations within helix I of Twist1 result in distinct limb defects and variation of DNA binding affinities. Journal of Biological Chemistry. 2007; 282:27536–27546. [PubMed: 17652084]

Grieshammer U, Minowada G, Pisenti JM, Abbott UK, Martin GR. The chick limbless mutation causes abnormalities in limb bud dorsal-ventral patterning: implications for the mechanism of apical ridge formation. Development. 1996; 122:3851–3861. [PubMed: 9012506]

Hendershot TJ, Liu H, Clouthier DE, Shepherd IT, Coppola E, Studer M, Firulli AB, Pittman DL, Howard MJ. Conditional deletion of Hand2 reveals critical functions in neurogenesis and cell type-specific gene expression for development of neural crest-derived noradrenergic sympathetic ganglion neurons. Developmental Biology. 2008; 319:179–191. [PubMed: 18501887]

Hollenberg SM, Sternglanz R, Cheng PF, Weintraub H. Identification of a new family of tissue-specific basic helix-loop-helix proteins with a two-hybrid system. Mol Cell Biol. 1995; 15:3813–3822. [PubMed: 7791788]

Holler KL, Hendershot TJ, Troy SE, Vincentz JW, Firulli AB, Howard MJ. Targeted deletion of Hand2 in cardiac neural crest-derived cells influences cardiac gene expression and outflow tract development. Developmental Biology. 2010; 341:291–304. [PubMed: 20144608]

Johnson RL, Tabin CJ. Molecular models for vertebrate limb development. Cell. 1997; 90:979–990. [PubMed: 9323126]

Maska EL, Cserjesi P, Hua LL, Garstka ME, Brody HM, Morikawa Y. A Tlx2-Cre mouse line uncovers essential roles for hand1 in extraembryonic and lateral mesoderm. Genesis. 2010; 00:1–6.

McFadden DG, Barbosa AC, Richardson JA, Schneider MD, Srivastava D, Olson EN. The Hand1 and Hand2 transcription factors regulate expansion of the embryonic cardiac ventricles in a gene dosage-dependent manner. Development. 2005; 132:189–201. [PubMed: 15576406]

McFadden DG, Charite J, Richardson JA, Srivastava D, Firulli AB, Olson EN. A GATA-dependent right ventricular enhancer controls dHAND transcription in the developing heart. Development. 2000; 127:5331–5341. [PubMed: 11076755]

McFadden DG, McAnally J, Richardson JA, Charite' J, Olson EN. Misexpression of dHAND induces ectopic digits in the developing limb bud in the absence of direct DNA binding. Development. 2002; 129:3077–3088. [PubMed: 12070084]

Morikawa Y, Cserjesi P. Extra-embryonic vasculature development is regulated by the transcription factor HAND1. Development. 2004; 131:2195–2204. [PubMed: 15073150]

Morikawa Y, Cserjesi P. Cardiac Neural Crest Expression of Hand2 Regulates Outflow and Second Heart Field Development. Circ Res. 2008; 103:1422–1429. [PubMed: 19008477]

Morikawa Y, D'Autreaux F, Gershon MD, Cserjesi P. Hand2 determines the noradrenergic phenotype in the mouse sympathetic nervous system. Developmental Biology. 2007; 307:114–126. [PubMed: 17531968]

Red-Horse K, Ueno H, Weissman IL, Krasnow MA. Coronary arteries form by developmental reprogramming of venous cells. Nature. 464:549–553. [PubMed: 20336138]

Riley P, Anson-Cartwright L, Cross JC. The Hand1 bHLH transcription factor is essential for placentation and cardiac morphogenesis. Nat Genet. 1998; 18:271–275. [PubMed: 9500551]

Soriano P. Generalized lacZ expression with the ROSA26 Cre reporter strain. Nat Genet. 1999; 21:70–71. [PubMed: 9916792]

Srinivas S, Watanabe T, Lin CS, William CM, Tanabe Y, Jessell TM, Costantini F. Cre reporter strains produced by targeted insertion of EYFP and ECFP into the ROSA26 locus. BMC Developmental Biology. 2001; 1:4. [PubMed: 11299042]

NIH-PA Author Manuscript

NIH-PA Author Manuscript

NIH-PA Author Manuscript

Srivastava D, Cserjesi P, Olson EN. A subclass of bHLH proteins required for cardiac morphogenesis. Science. 1995; 270:1995–1999. [PubMed: 8533092]

Vincentz JW, BArnes RM, Rodgers R, Firulli BA, Conway SJ, Firulli AB. An Absence of Twist1 results in aberrant cardiac neural crest morphogenesis. Dev Biol. 2008; 320:131–139. [PubMed: 18539270]

Yanagisawa H, Clouthier DE, Richardson JA, Charite J, Olson EN. Targeted deletion of a branchial arch-specific enhancer reveals a role of dHAND in craniofacial development. Development. 2003; 130:1069–1078. [PubMed: 12571099]

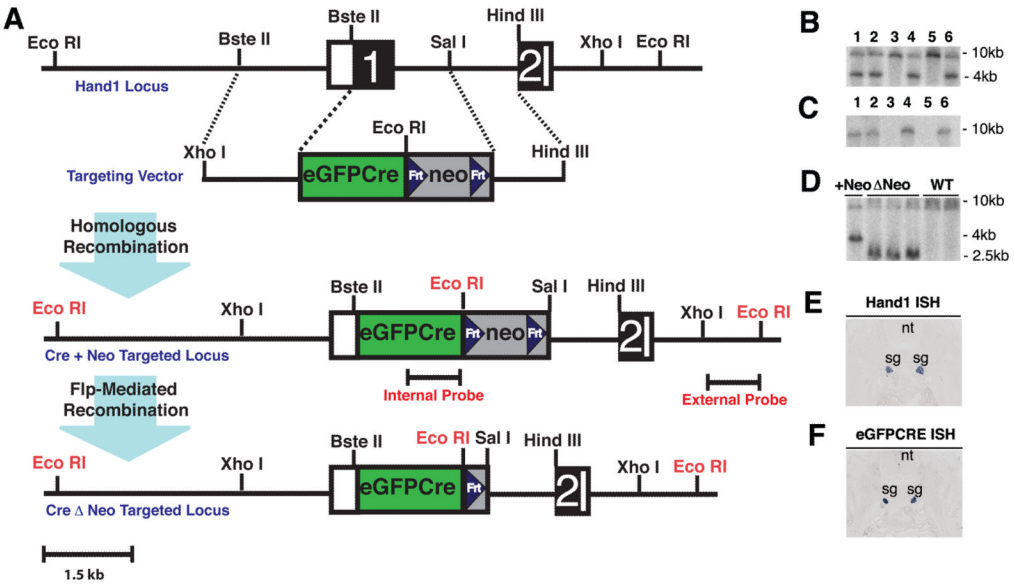

Figure 1.

Generation and validation of the *Hand1*^{eGFPCre} mouse line. A) The *Hand1* locus is shown at the top with non-coding and coding regions indicated by the white and numbered-black boxes, respectively. The targeting vector is shown below with the dotted lines indicating regions of sequence identity between the targeting arms. The targeting strategy introduced an *eGFPCre* cassette into the 5' untranslated region of *Hand1*, followed by an *FRT*-flanked *PGK-neo*. Homologous recombination resulted in deletion of the first exon of *Hand1* and insertion of the *eGFPCre* gene under control of the endogenous promoter. Following germline transmission of the mutation, the *PGK-neo* was deleted by subsequent mating with the *FLPeR* mouse line. B) Southern blot of *Hand1*$^{eGFPCre+Neo/+}$ offspring using an external probe to detect the targeted allele and C) using an internal probe to confirm the absence of transgenic incorporation of the targeting construct. D) Southern blot of *Hand1*$^{eGFPCreΔNeo/+}$ offspring following *Flp Recombinase* mediated deletion of the *PGK-neo*. (E, F) RNA *in situ* hybridization on E13.5 *Hand1*$^{eGFPCreΔNeo/+}$ embryos shows identical tissue-specific *Hand1* and *eGFPCre* expression.

NIH-PA Author Manuscript NIH-PA Author Manuscript NIH-PA Author Manuscript

NIH-PA Author Manuscript

NIH-PA Author Manuscript

NIH-PA Author Manuscript

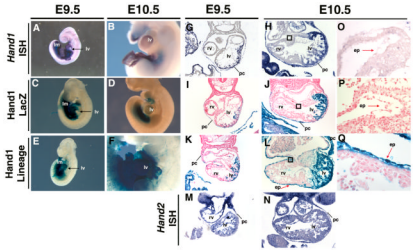

Figure 2.

The *Hand1*-Lineage contributes to a subset of the first heart field and epicardium. DIG-labeled whole-mount (A, B) and transverse section (G, H, O) *in situ* hybridization for *Hand1* on wild-type embryos at E9.5 and E10.5. LacZ staining of the *Hand1*^{LacZ} (C, D, I, J, P) and *Hand1*^{eGFPCre} lineage (E, F, K, L, Q). Boxed regions are shown in magnification (O,P,Q). Black Arrow denotes the left ventricle while the red arrow denotes to the epicardium. ep, epicardium; lm, lateral mesoderm; lv, left ventricle; pc, pericardium; rv, right ventricle.

NIH-PA Author Manuscript

NIH-PA Author Manuscript

NIH-PA Author Manuscript

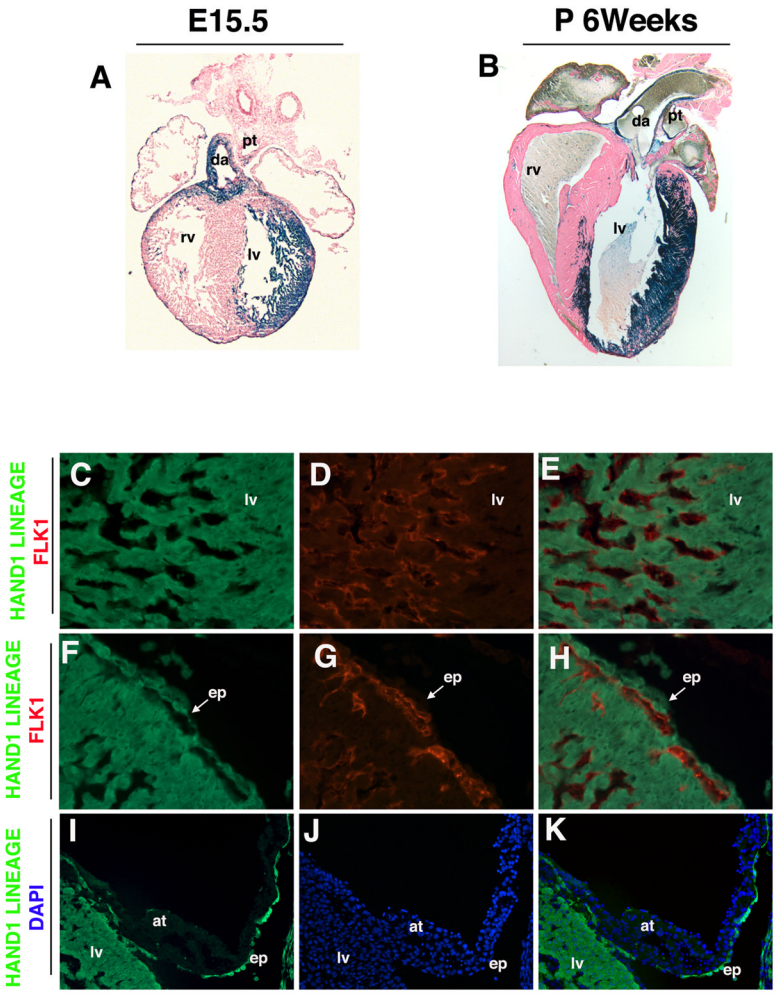

Figure 3.

Analysis of the adult *Hand1* lineage shows restriction to specific cardiovascular lineage subsets. LacZ staining of *Hand1*-lineage cryosections (A, B). E13.5 immunohistochemistry for Flk1 (red; D, G) and the *Hand1*-lineage (green; C, F). Overlay of Flk1 and the *Hand1*-lineage (E, H). E13.5 immunohistochemistry for the *Hand1*-lineage (green; I) counterstained with DAPI (blue; J). Overlay for DAPI and the *Hand1*-lineage (K). at, atria; da, dorsal aorta; ep, epicardium; lv, left ventricle; pt, pulmonary trunk; rv, right ventricle.

NIH-PA Author Manuscript

NIH-PA Author Manuscript

NIH-PA Author Manuscript

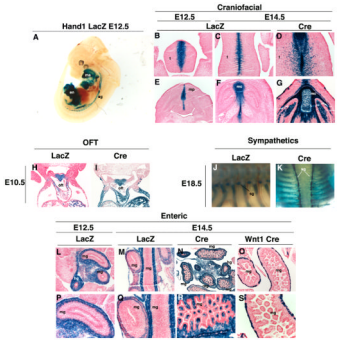

Figure 4.

The *Hand1*-lineage marks discrete neural crest cell populations. Whole-mount LacZ staining of *Hand1*^{LacZ} (A,J) and the *Hand1*-lineage (K). Transverse sections of whole mount LacZ stained *Hand1*^{LacZ} (F) and *Hand1*-lineage (G) embryos. LacZ staining of *Hand1*^{LacZ} (B, C, E, F, L, M, P, and Q), *Hand1*-lineage (D, G, N, and R), and *Wnt1*-lineage (O,S) cryosections. en, enteric; hg, hindgut; ma, mandible; mc, meckel's cartilage; mg, midgut; mp, mandibular process; oft, outflow tract; pv, posterior vein; sg, sympathetic ganglia; t, tongue.

NIH-PA Author Manuscript

NIH-PA Author Manuscript

NIH-PA Author Manuscript

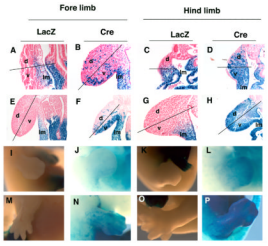

Figure 5.

Analysis of the *Hand1* limb lineage. LacZ Staining of *Hand1*^{LacZ} and the *Hand1* lineage at E9.5 (A–D), E10.5 (E–H), E12.5 (I–L), and E14.5 (M–P). Transverse sections of LacZ stained embryos showing fore and hind limbs (A–H). Whole-mount LacZ staining (I–P). d, dorsal; lm, lateral mesoderm; v, ventral.

NIH-PA Author Manuscript

NIH-PA Author Manuscript

NIH-PA Author Manuscript

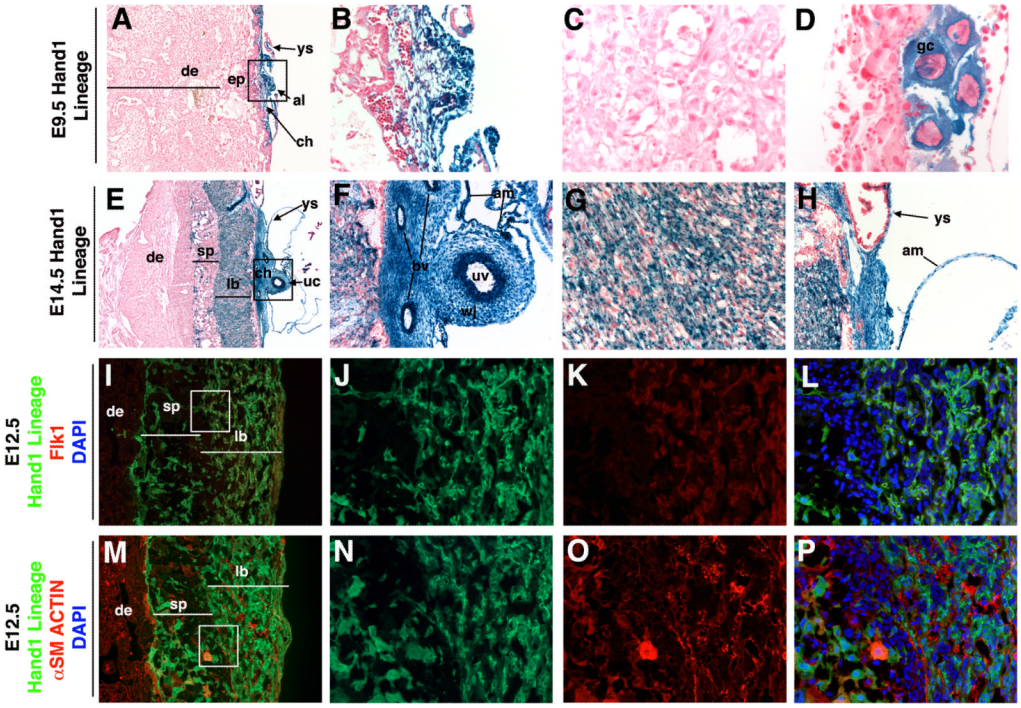

Figure 6.

The *Hand1* lineage contributes to the EEM and Trophoblasts during placental development. LacZ staining of *Hand1*-lineage cryosections (A–H). Immunohistochemistry for the *Hand1*-lineage (green; I, J, M, N), Flk1 (red; K), αSM-Actin (red; O). Overlay for the *Hand1* lineage, Flk1, and DAPI (blue; L). Overlay for the *Hand1* lineage, and αSM-Actin, DAPI (blue; P). al, allantois; am, amnion; ch, chorion; de, decidua; ep, ectoplacental plate; gc, giant cell; lb, labyrinth; sp spongiotrophoblast; uc, umbilical chord; uv, umbilical vessels; ys, yolk sack; wj, Wharton's jelly.

NIH-PA Author Manuscript

NIH-PA Author Manuscript

NIH-PA Author Manuscript

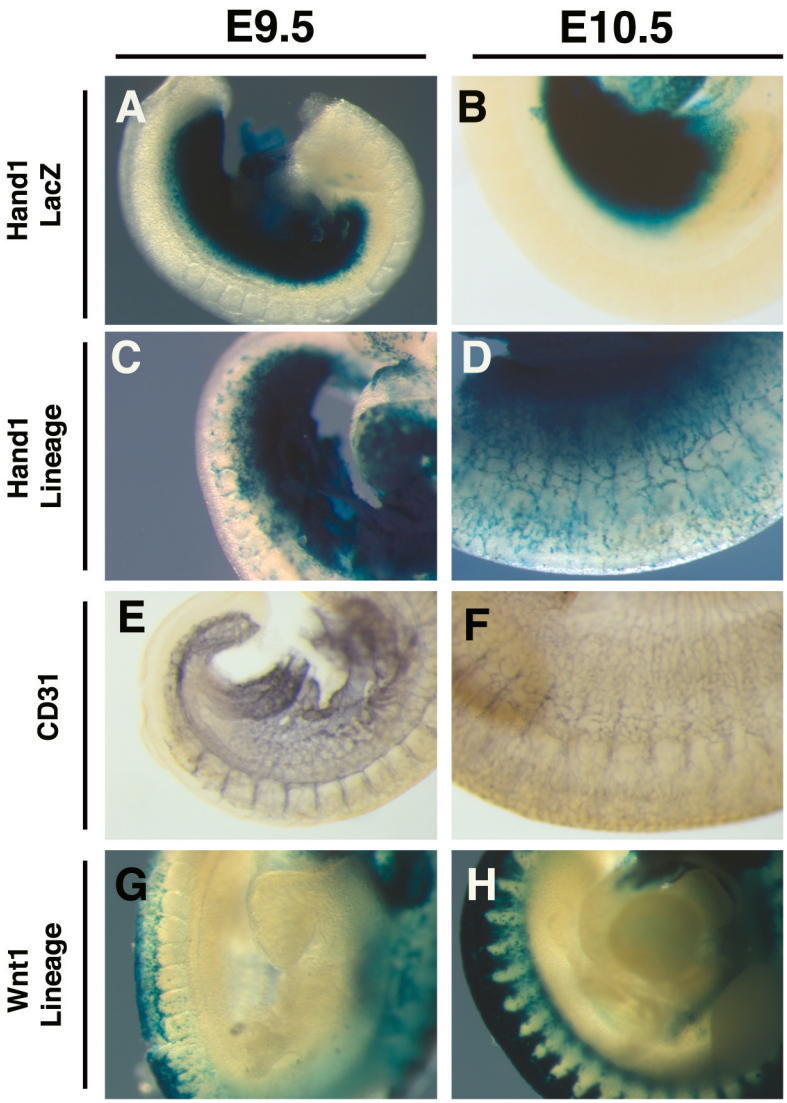

Figure 7.

Lateral mesodermal derivatives of the *Hand1* lineage gives rise to intussuceptive microvascular growth. Whole-mount LacZ staining of the *Hand1*^{LacZ} (A, B), the *Hand1*-lineage (C, D), and the *Wnt1*-lineage (G, H). Whole-mount antibody staining for CD31 (E, F).

NIH-PA Author Manuscript

NIH-PA Author Manuscript

NIH-PA Author Manuscript

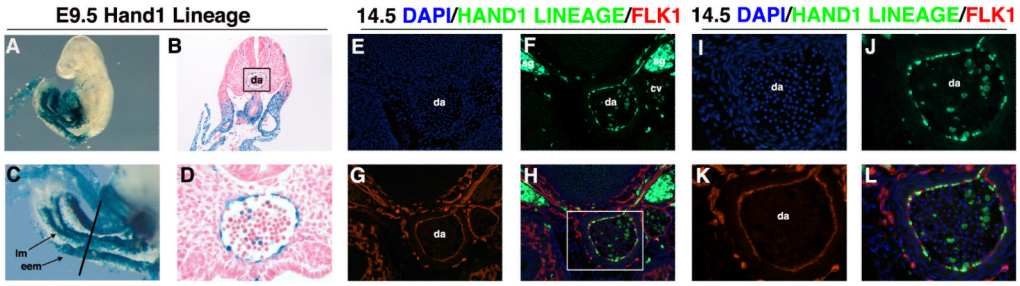

Figure 8.

Lateral mesodermal derivatives of the *Hand1* lineage give rise to endothelial progenitors of the dorsal aorta. Whole-mount LacZ staining of the *Hand1*-lineage (A, C). Transverse sections of whole mount LacZ stained *Hand1*-lineage embryos (B, D). Immunohistochemistry for the *Hand1*-lineage (green; F, J), Flk1 (red; G, K), and DAPI nuclear staining (blue; E, I). Overlay for the *Hand1*-lineage, Flk1, and DAPI (H, L). cv, cardinal vein; da, dorsal aorta; eem, extraembryonic mesoderm; lm, lateral mesoderm; sg, sympathetic ganglia.